

A Model to Realize the Potential of Auger Electrons for Radiotherapy

B. Q. Lee^{1,a}, T. Kibédi¹, A. E. Stuchbery¹, K. A. Robertson¹, and F. G. Kondev²

¹Department of Nuclear Physics, The Australian National University, ACT 0200, Australia

²Nuclear Engineering Division, Argonne National Laboratory, Argonne, Illinois 60439, USA

Abstract. Auger-electron-emitting radioisotopes provide a unique tool that enables the targeted irradiation of a small volume in their immediate vicinity. Over the last forty years, Auger emission has been established as a promising form of molecular radiotherapy, and it has recently made the transition from the laboratory to the clinic. In this paper we review the physical processes of Auger emission in nuclear decay and present a new model being developed to evaluate the energy spectrum of Auger electrons from radioisotopes.

1 Introduction

Unstable atomic nuclei release excess energy through various radioactive decay processes by emitting radiation in the form of particles (neutrons, alpha and beta particles) or electromagnetic radiation (photons). Most of the applications of nuclear isotopes make use of the fact that the interaction of the radiations passing through a material depend on their type (photons, neutral or charged particles) and their energy.

Alpha and beta particles are two well known ionizing radiations. Most radioisotopes used in clinical therapy emit β particles. A new class of α -emitting radioisotopes [1], including ^{211}At , ^{213}Bi , ^{213}Po , ^{223}Ra , and ^{225}Ac , have been considered for therapy. Auger electrons are a third type of ionizing radiation [2], named after the French physicist Pierre Victor Auger. When an inner-shell electron is removed from an atom, the vacancy will be filled by an electron from the outer shells and the excess energy will be released as an X-ray photon, or by the emission of an Auger electron. Referred to as atomic radiations, X-ray and Auger-electron emission are competing processes. The atomic transition rate and the energy of emitted X-rays and/or Auger electrons depend on the atomic number, the electron shells involved, and the electronic configuration of the atom. The full relaxation of an inner-shell vacancy is a multi step process, resulting in a cascade of atomic radiations. The energy of each atomic radiation is typically in the range from a few eV up to hundreds of keV.

Auger electron therapy is a promising form of molecular radiotherapy that has recently made the transition from the laboratory to the clinic [3, 4]. A term has been coined, targeted radioimmunotherapy (tRIT), to emphasize the unique characteristics of the short range but highly toxic, Auger electrons. The benefits of Auger-electron based therapies and the current understanding of the physical behavior of Auger electrons in cells and DNA have

recently been reviewed by Cornelissen and Vallis [4] and Kassis [5].

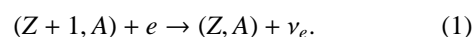
Comparatively, progress in theoretical modelling of the Auger cascade has been slow and leading researchers have expressed their concerns regarding the accuracy of the existing Auger-electron spectrum calculations [6]. Recently published papers still refer to calculations published decades ago, even though a new sophisticated tool to evaluate internal conversion coefficients, BrIcc [7] has been made available. Internal conversion often initiates the Auger cascade in radioisotopes. Therefore, it is important to revisit the evaluation of the Auger cascade and build new computational models to calculate Auger-electron spectra based on up-to-date nuclear data.

In this paper we will focus on the physical processes required to evaluate Auger emission in nuclear decay. We start our discussion with an overview of the current knowledge. We then propose a new approach to overcome the limitations of the previous computations of low-energy Auger emission from medical isotopes.

2 Radioactive decay processes

When a vacancy is created in an inner electron shell, the residual atom is left in an excited state. Such a vacancy can be created by electron capture (EC) or by the emission of internal conversion electrons (CE) after nuclear decay.

In electron capture, the nucleus decays by absorbing an atomic electron and emitting a neutrino:



The condition for electron capture decay is

$$E_\nu = Q^+ - E_i - E_X > 0, \quad (2)$$

where Q^+ is the energy difference in atomic masses between parent and daughter ground states, E_i is the energy of the final nuclear state in the daughter nucleus, and E_X

^ae-mail: boon.lee@anu.edu.au

is the binding energy of the captured electron, X . The released energy, E_ν will be shared by the emitted neutrino and, if applicable, the bremsstrahlung photon or shake-off electron. A comprehensive compilation of the relevant electron capture probability ratios for the K , L , M , N and O shells has been presented by Schönfeld [8].

Nuclei undergoing electromagnetic decays will emit γ -rays, internal conversion electrons, or if the transition energy is higher than twice the electron rest mass, electron-positron pairs. In the internal conversion process an atomic electron is ejected from one of the atomic shells. The electron conversion coefficient is defined as the ratio of the probabilities for the emission of atomic electrons from a shell X (P_X) to the emission of γ -rays (P_γ):

$$\alpha_X = \frac{P_X}{P_\gamma}. \quad (3)$$

3 X-rays and Auger electrons

It is customary to assume that the radioactive atom initially is in the neutral, ground-state electronic configuration. Immediately after an electron capture or internal conversion event, the atom will be excited by the removal of an inner electron. In 1923, S. Rosseland [9] postulated that the atom relaxes via both radiative and non-radiative processes. Radiative processes involve the emission of X-rays with characteristic energies as the atomic electrons are re-organized to fill the vacancy. In X-ray emission, an electron in an outer shell, Y , makes a transition to a vacancy in the inner shell, X , and the emitted energy of the X-ray is:

$$E_{XY} = E_{BE,X} - E_{BE,Y}, \quad (4)$$

where $E_{BE,X}$ and $E_{BE,Y}$ are the binding energies of the atomic shells involved. The fluorescence yield, ω_X , is defined as the number of radiative (X-ray) transitions per vacancy in any shell or subshell X . Considering all possible subshells, Y , that could be involved in filling a vacancy in the K -shell, the X-ray yield, Y_{KY} can be expressed as:

$$Y_{KY} = f_K \omega_K N_{KY}, \quad (5)$$

where f_K is the number of primary vacancies on the K -shell, and N_{KY} is the relative intensity of the various X-ray transitions with $\sum N_{KY} = 1$.

Lise Meitner and Pierre Auger made independent experimental observations of the non-radiative process in 1922 [10] and 1925 [2]. Non-radiative processes similarly involve the redistribution of atomic electrons but result in the emission of an atomic electron (Auger electron) rather than a photon. The Auger electron process XYZ involves three electron subshells. An electron in an outer shell, Y , makes a transition to the vacancy in an inner shell, X , and an electron in outer shell Z is ejected. The energy of the Auger electron can be expressed as:

$$E_{XYZ} = E_{BE,X} - E_{BE,Y} - E_Z^Y, \quad (6)$$

where $E_{BE,X}$ and $E_{BE,Y}$ are the neutral atom binding energies for shell X and Y . E_Z^Y is the binding energy of an electron on the Z -shell when the atom is already ionized with

a single vacancy on the atomic shell Y . This process will result in secondary vacancies in both the Y and Z shells from a single primary vacancy in the X shell. Similarly to Eqn. 5, the Auger electron yield can be expressed as:

$$Y_{KYZ} = f_K(1 - \omega_K)N_{KYZ}, \quad (7)$$

where N_{KYZ} is the relative intensity of various Auger transitions with $\sum \sum N_{KYZ} = 1$. The sums are over all energetically possible Y and all possible Z with binding energies $E_{BE,Y} \geq E_{BE,Z}$.

4 Vacancy propagation

The rearrangement of the atomic structure will continue until all primary, secondary and subsequent vacancies are filled by the emission of X-rays and Auger electrons, or until no more transitions are energetically possible. In the latter case, the vacancies have reached the valence shells.

The full relaxation of the initial vacancy created by the nuclear event (section 2) is a multi step process known as ‘‘vacancy propagation’’ or the ‘‘Auger-electron cascade’’. Vacancy propagation is generally accepted to have a very short time scale of 10^{-16} to 10^{-14} s. While the fundamental physical picture of the individual atomic transitions remains similar to the one described above, the atomic structure will continuously change. This change will affect both the atomic binding energies and the transition rates.

Table 1 compares the present and previous calculated Auger electron yields of six medically important radioisotopes, namely ^{99m}Tc , ^{111}In , $^{123,125}\text{I}$, ^{131}Cs , and ^{201}Tl . The calculations follow two fundamentally different approaches to evaluate the vacancy propagation, designated ‘deterministic’ and ‘Monte Carlo’. A detailed review of these two approaches has been given elsewhere [11, 12]. In the following we discuss the new model which is based on the Monte Carlo method.

5 New ab initio calculations of the Auger energy spectrum - A pilot study

The starting point to explore the potential of targeted Auger electron-based therapy is an accurate description of the relevant atomic radiation spectrum from the nuclear decay of candidate radioisotopes. Recognizing the lack of a consistent theoretical model for this purpose, the August 2011 IAEA special meeting on Intermediate-term Nuclear Data Needs for Medical Applications [21] concluded that: ‘‘A comprehensive calculational route also needs to be developed to determine the energies and emission probabilities of the low-energy X-rays and Auger electrons to a higher degree of detail and consistency than is available at present.’’ To improve the understanding of the atomic radiation spectra in nuclear decay, a new approach is required, which should use new theoretical transition energies and rates. In addressing this need we propose a protocol for a new Monte Carlo approach. A detailed description and some preliminary results have been given elsewhere [11, 12]; here only the main aspects are summarized.

Table 1. Calculated Auger electron yield per nuclear decay for selected medical radioisotopes.

	RADAR ^a	DDEP ^a	Eckerman & Endo ^a	Howell ^b	Stepanek ^b	Pomplun ^b	Nikjoo ^b	Present study ^b
	[13, 14]	[15]	[16]	[17]	[18]	[19, 20]	[6]	
^{99m} Tc (6.007 h)	0.122	0.13	4.363	4.0		2.5		3.34
¹¹¹ In (2.805 d)	1.136	1.16	7.215	14.7	6.05			5.75
¹²³ I (13.22 h)	1.064	1.08	13.71	14.9		6.4		6.81
¹²⁵ I (59.4 d)	1.77	1.78	23.0	24.9	15.3	12.2	20.2	10.9
¹³¹ Cs (9.689 d)	0.4745		10.7					6.22
²⁰¹ Tl (3.04 d)	0.773	0.614	20.9	36.9				11.9

^a Deterministic^b Monte Carlo

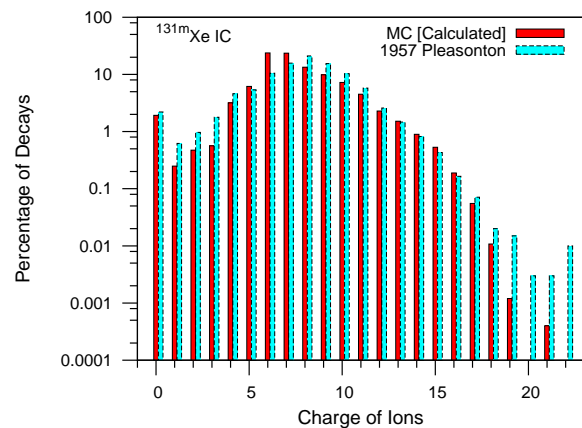
Firstly, nuclear structure data will be extracted from the Evaluated Nuclear Structure File (ENSDF) [22]. ENSDF is maintained regularly and this will ensure the use of up-to-date information to evaluate the nuclear event.

Secondly, electron capture rates will be taken from the Schönfeld (1995) compilation [8]. Internal conversion coefficients (ICC) will be taken from *BrIcc* [7]. The ICC values in that tabulation were calculated using relativistic Dirac-Fock wave functions.

Thirdly, Auger and X-ray transition energies and rates will be calculated using the most recent version of the General Purpose Relativistic Atomic Structure Program, GRASP2K [23] and the Relativistic Atomic Transition and Ionization Properties, RATIP [24] codes. This approach will use the relativistic multiconfiguration Dirac-Fock (MCDF) method. The RATIP program package was developed in the late 90s for the calculation of atomic transition and ionization properties for charged ions [25], similar to those expected during the vacancy propagation process. Calculations will be carried out at every propagation step for the actual atomic configuration of the ionized atom.

In all practical cases CE takes place *after* the daughter atom is fully relaxed following an EC event, so internal conversion takes place in a neutral atom. Thus the vacancy creation and the atomic relaxation processes from EC decay and from internal conversion will be treated independently.

An *ab initio* treatment of the propagation process, including the random sampling of the available decay channels, will ensure a realistic evaluation of the atomic spectra. In this approach the atom is assumed to be free, and any influence from the chemical environment or solid state effects are neglected. In our model, the propagation of a particular vacancy will be terminated once there is no higher level with an electron energetically available to fill the vacancy. The propagation of the initial event is complete once all vacancies have reached the outermost shell. In the proposed model it will be assumed that the vacan-

**Figure 1.**

Comparison of calculated (pilot model) and observed charge distribution after de-excitation of ^{131m}Xe. The shakeoff process is included in the calculations. The calculated Auger yield for ^{131m}Xe is 5.20 per decay. The shakeoff probability for every subshell in xenon is obtained from [26]. The experimental charge distribution labelled as 1957 Pleasonton is from [27].

cies on the valence shell(s) will remain unfilled throughout the relaxation process.

To explore the implications of this new approach, a pilot model was developed. This model follows the proposed approach, except that fixed atomic transition rates were taken from the Livermore Evaluated Atomic Data Library (EADL) [29] data base. Transition energies for every possible electronic configuration were deduced from binding energies given by the RAINE Dirac-Fock code [30], and transitions with negative energies were excluded.

Calculated Auger electron yields for selected medical isotopes are shown in Table 1. The main uncertainties in the evaluation process come from the EADL data base and the RAINE program. The EADL data base does not specify the uncertainties in the calculations, and theoretical neutral binding energies from RAINE diverge from

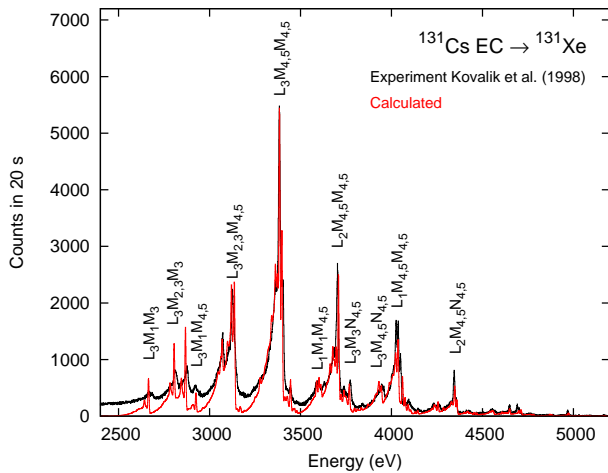


Figure 2. Calculated LMM+LMX+LXY Auger energy spectrum of ^{131}Xe is compared to the experimental spectrum from [28]. The line shape of the experimental spectrum has been folded into the calculated spectrum.

empirical values by up to about 1%. In accord with our assumption that valence-shell vacancies persist, our results are consistent with those of Pomplun [19, 20]. We have therefore demonstrated that we can reproduce the previous Monte Carlo calculations for these isotopes.

Figure 1 demonstrates good agreement between the calculated and experimental charge distribution following de-excitation of ^{131m}Xe . It is evident that the internal conversion process that usually accompanies the decay of ^{131m}Xe usually leaves the atom in a highly ionized state, even though only a single initial vacancy is created by the nuclear process.

The calculated L Auger energy spectrum of ^{131}Xe following EC decay of ^{131}Cs as compared with the measured spectrum shows good agreement in terms of the shape of the spectrum, the locations of the Auger peaks, and the heights of each peak (Figure 2). The few exceptions are the $L_3M_{2,3}M_3$ and $L_3M_1M_3$ Auger groups. The shapes and locations of these groups agree well with the experiment but the calculated intensities of these groups are slightly higher than the observed values.

Figure 3 compares the calculated and experimental KLL Auger spectra of ^{131}Xe . Calculated energies of the KLL group are higher than the observed values because theoretical binding energies from RAINE neglect QED corrections. Also, the calculated spectrum does not contain the splitting of several lines because EADL transition rates were calculated with the $j-j$ coupling scheme instead of the intermediate coupling - configuration interaction (IC-CI) coupling scheme. For atoms $Z \leq 60$, IC-CI coupling is necessary.

In summary, the pilot model has thus far proved to be a useful tool in predicting Auger energy spectra and charge distributions of residual ions following nuclear decays. We do not expect it will achieve perfect agreement with all experimental results. For example, the disagreements between the model and experiment for KLL Auger electrons signifies that our work is not complete. How-

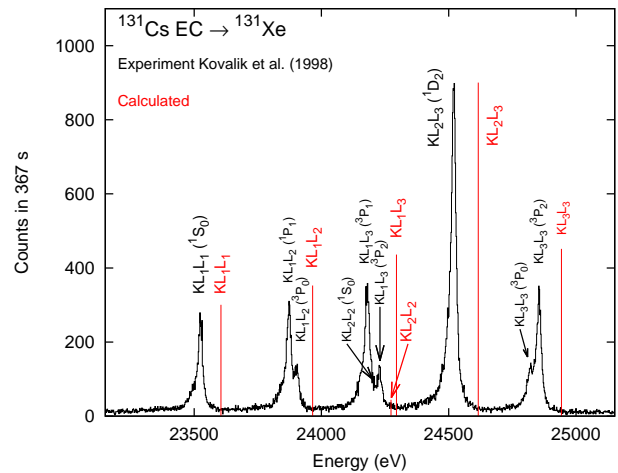


Figure 3. Calculated KLL Auger electron energy spectrum of ^{131}Xe is compared to the experimental spectrum from [28].

ever we understand the reasons for these discrepancies between theory and experiment. The pilot model will be the cornerstone for our future work using GRASP2K [23] and RATIP [24] to evaluate more accurate atomic transition rates and electron configuration energies.

6 Conclusions

Auger-electron-emitting radioisotopes provide a unique source of ionizing radiation. Due to their low energy and short range, Auger electrons damage only a small volume in their immediate vicinity. This unique characteristic encourages continuing interest in medical applications of Auger electrons, particularly for targeted tumor therapy. In most cases these applications are based on theoretical predictions of the emitted Auger and X-ray spectra. As is evident from Table 1, there is a significant difference in the calculated Auger yields reported in the literature over the last 20 years. Most of these differences can be attributed to the lack of detailed knowledge of the relevant atomic transition rates, most importantly in the outer (M , N , etc.) shells. Simplistic assumptions regarding the atomic configurations during vacancy propagation, and the incomplete treatment of the effect of multiple vacancies, also limit the validity of these predictions.

We are developing a new model for Auger electron spectra using *ab initio* calculations based on the relativistic MCDHF method and Monte Carlo techniques, which has the potential to overcome these limitations. The pilot model based on fixed transition rates from the EADL [29] produces results that are in good agreement with the experiments for the energy spectrum of L Auger groups and charge state distribution of residual atoms.

Acknowledgements

The authors are much indebted to Dr. A. Kovalík and Dr. A. Inoyatov from the Laboratory of Nuclear Problems, Dubna, for providing the experimental data of Auger energy spectra in Figure 2 and 3. Work at ANL was sup-

ported by the U.S. Department of Energy, Office of Nuclear Physics, under Contract No. DE-AC02-06CH11357.

References

- [1] G. Sgouros, *Adv. Drug Deliver. Rev.* **60** (2008) 1402
- [2] P. Auger, *J. de Physique et le Radium* **6** (1925) 205
- [3] X. Liu *et al*, *J. Nucl. Med.* **50** (2009) 582
- [4] B. Cornelissen *et al*, *Curr. Drug Discov. Tech.* **7** (2010) 263
- [5] A. Kassis, *Radiat. Prot. Dosim.* **143** (2011) 2
- [6] H. Nikjoo *et al*, *Int. J. Radiat. Biol.* **84** (2008) 1011
- [7] T. Kibédi *et al*, *Nucl. Instr. and Meth. in Phys. Res. A* **589** (2008) 202
- [8] E. Schönfeld, *Appl. Radiat. Isot.* **49** (1998) 1353
- [9] R. Rosseland, *Zeitschrift für Physik A Hadrons an Nuclei* **14** (1923) 17
- [10] L. Meitner, *Zeitschrift für Physik* **9** (1922) 131
- [11] B. Lee *et al*, *Comput. Math. Meth. Med.* **14** (2012) 651475
- [12] B. Lee *et al*, *Eur. Phys. J.: Web of Conferences* **35** (2012) 04003
- [13] RADiation Dose Assessment Resource (RADAR), <http://www.doseinfo-radar.com/RADARHome.html>.
- [14] M.G. Stabin, L.C. da Luz, *Health. Phys.* **83** (2002) 471
- [15] Decay Data Evaluation Project, http://www.nucleide.org/DDEP_WG/DDEPdata.htm, ^{99m}Tc: C. Morillon, M.M. Bé, A. Egorov (2012); ¹¹¹In: V.P. Chechev (2006); ¹²³I: V. Chiste, M.M. Bé (2004); ¹²⁵I: V. Chiste, M.M. Bé (2010); ²⁰¹Tl: E. Schönfeld, R. Dersch (2005).
- [16] K.F. Eckerman *et al*, *Society of Nuclear Medicine* (2007)
- [17] R.W. Howell, *Med. Phys.* **19** (1992) 1371
- [18] J. Stepanek, *Med. Phys.* **27** (2000) 1544
- [19] E. Pomplun, *Acta Oncol.* **39** (2000) 673
- [20] E. Pomplun, *Int. J. Radiat. Biol.* **88** (2012) 108
- [21] Summary Report of the “Technical Meeting on Intermediate-term Nuclear Data Needs for Medical Applications: Cross Sections and Decay Data”, INDC International Nuclear Data Committee, Eds. A.L. Nichols, S.M. Qaim, R.C. Noy, INDC(NDS)-0596, September 2011.
- [22] Evaluated Nuclear Structure Data File (ENSDF), NNDC, BNL <http://www.nndc.bnl.gov/ensdf/index.jsp>
- [23] P. Jönsson *et al*, *Comp. Phys. Comm.* **177** (2007) 597
- [24] J. Nikkinen *et al*, *Comp. Phys. Comm.* **175** (2006) 348
- [25] M. Patanen *et al*, *Phys. Rev. A* **83** (2011) 053408
- [26] T. Carlson *et al*, *Phys. Rev. A* **8** (1973) 2887
- [27] F. Pleasonton *et al*, *Sciences* **241** (1957) 141
- [28] A. Kovalík *et al*, *J. Electron Spectrosc.* **95** (1998) 231
- [29] S.T. Perkins *et al*, *Lawrence Livermore National Laboratory, UCRL-50400* **30** (1991)
- [30] I.M. Band *et al*, *At. Data and Nucl. Data Tables* **81** (2002) 1